

Wideband Lamb wave analysis based on continuous wavelet transform

Lihua Shi[†]

*Laboratory of Electromagnetics, Nanjing Engineering Institute,
No.1 Haifuxiang, Nanjing 210007, China*

Xinwei Wang[‡] and Gang Li^{‡†}

*The Aeronautical Science Key Laboratory for Smart Materials and Structures,
Nanjing University of Aeronautics and Astronautics, Nanjing 210016, China*

Lingyan Zhang^{**}

*Laboratory of Electromagnetics, Nanjing Engineering Institute, Nanjing 210007, China
(Received August 30, 2004, Accepted April 29, 2005)*

Abstract. In Lamb wave detection of damages in smart structures, the excitation pulse is usually designed as a narrow band burst wave for the convenience of analysis and recognition. However, the wideband excitation can excite more modes in plate/shell structure and thus provides extra information for changes of the structure. This paper presents a method that can extract information in wideband Lamb wave signals. By transforming the detected signals into various sub-frequency band, the measured signal can be converted to its equivalences of narrow band excitations, therefore, the information in different frequency bands can be acquired from a single test and in the same time the complicity of wideband signal can be simplified. Some test results are provided to verify this method.

Keywords: Lamb wave, wavelet transform, time-frequency analysis, damage detection, dispersion

1. Introduction

Health monitoring of structures by using ultrasonic Lamb wave has received great attention in the field of smart materials and structures recently. The idea of Lamb wave damage detection is to launch an elastic guided wave at one position and measuring the arrived wave at another position after the wave acts with the structure along the propagation path. Because the Lamb wave can travel a long distance along the plate or shell structure, it is possible to scan an entire range of structure without moving probes during the inspection, saving greatly in inspection time and cost. Conventional Lamb wave transducers use an angled wedge to efficiently couple ultrasonic energy into the material under

[†]Professor and Director, E-mail: Shilh@jlonline.com

[‡]Professor and Deputy Director, E-mail: wangx@nuaa.edu.cn

^{‡†}Ph.D Student, E-mail: ligangdy@public.zj.js.cn

^{**}Graduated Student, E-mail: stone712@yahoo.com

investigation (Alleyne and Cawley 1992). In Smart material structures, a built-in transducer system consists of PZT sensor array used for onsite monitoring (Lin and Chang 2002). Because of the intrinsic characteristics of stress wave propagating in thin plates, there could be multi-modes existing in the tested structure, such as symmetric mode S_0, S_1, \dots and anti-symmetric mode A_0, A_1, \dots (Vikto 1970). The variation of Lamb wave propagation speed with modes and frequency causes dispersion fact in the structure and makes the final detected waveform have complicated shapes. The key point in Lamb wave detection is to get a clear signal without too much dispersion and reflections. In this case, the low frequency excitation signal is preferred, as for low frequency-thickness product, only two fundamental modes will occur (Cawley 1997). In order to reduce the dispersion effect and improve the localization accuracy, a frequency-domain and time-domain localized windowed sine wave function (the burst wave) is often selected as the input signal. There have been some articles discussing the optimization of Lamb wave based method for damage detection in composite materials (Alleyne and Cawley 1992, Wilcox, *et al.* 1999, Kessle, *et al.* 2001). Due to the characteristics of various embedded transducers and the actual circumstance of materials/structures, it is hard to find a good direction currently for designing the Lamb wave and selecting the frequency in real applications.

Besides the factors of transducers and excitation signals, Lamb wave detection and damage recognition rely also on the analyzing method. Many signal processing methods have been used, which include time-domain method, frequency domain method and time-frequency joint analysis. In the analysis of the narrow-band burst signal, the amplitude, phase/group delay and energy has been used to describe the features of damages (Ihn and Chang 2001). Wavelet transform (Lemistre and Balageas 2001), Wigner-Ville distribution (Prosser and Seale 1999) and short-time Fourier transform were used to analyze the frequency content at different time. The essence of these time-frequency analysis methods is to use a band pass filter to observe the information in the original time-history. In order to observe the dispersion effect of the Lamb wave, it is proposed to use the 2-D FFT to measure the dispersion curve from experimental data (Alleyne and Cawly 1991). The phase unwrapping method was also employed to get the phase velocity of the disperse signals (Ellefsen, Cheng and Tubman, 1989). In resent years, a new non-stationary signal analysis method, called Hilbert-Huang transform (HHT), begins to be used in Lamb wave analysis (Chen, Li and Teng 2002).

From the authors' point of view, the existing time-frequency analysis methods work well for wideband signals. For the narrow band signal, however, the frequency domain discrimination of them is not very good. Therefore, ideally, the Lamb wave detection approach should use a wideband inspection signal to observe the changes of multi-mode signals caused by damages. If only one burst wave at a fixed frequency is made, it might not contain enough information for damage diagnosis. To observe the sub-frequency band signal from the wideband signal, split spectrum method (Newhouse and Bilgutay 1982) and continuous wavelet (CWT) (Abbate and Frankel Das 1995) can be used. Xu, *et al* (2002) discussed the relationship between the narrow-band and wideband test results in electromagnetic measurement of concrete dielectric constant. This method is applied to Lamb wave detection in this paper. From the wide band measurement, the response of structure to narrow band burst wave can be acquired by a modified continues wavelet analysis method. Consequently the dispersion effect can be displayed by using a magnitude-time-frequency plot.

2. Continuous wavelet transform and band-pass filtering

If a compact-supported function $\psi(t)$ in $L^2(R)$ satisfies the admissible function condition,

$$C_\psi = \int_{-\infty}^{+\infty} \frac{|\Psi(\omega)|^2}{|\omega|^2} d\omega < \infty \quad (1)$$

where

$$\Psi(\omega) = \int_{-\infty}^{+\infty} \psi(t) e^{-j\omega t} dt \quad (2)$$

it can be used as an analytical function in the continuous wavelet transform (CWT). For a finite energy function $f(t)$, its CWT is defined as

$$W_\psi f(a, b) = \frac{1}{\sqrt{a}} \int_{-\infty}^{\infty} f(t) \bar{\psi}\left(\frac{t-b}{a}\right) dt \quad (3)$$

where $a > 0$ is called the scale factor, b is the time-shift and $\bar{\psi}(t)$ denotes the complex conjugate of $\psi(t)$.

Furthermore, by changing the original wavelet function into

$$g_a(t) = \frac{1}{\sqrt{a}} \bar{\psi}\left(-\frac{t}{a}\right) \quad (4)$$

the wavelet transform in Eq. (3) can be written as a filtering operation

$$W_g f(a, b) = \int_{-\infty}^{\infty} f(t) g\left(\frac{b-t}{a}\right) dt = f(t) * g_a(t) \quad (5)$$

where $*$ denotes the convolution.

Fig. 1 is the waveform and spectrum of a Morlet wavelet. It shows that the wavelet acts like a band-pass filter selecting certain frequency band from the analyzed signal for observation. In order to give an explicit frequency factor in CWT analysis, a modified Morlet wavelet is used in this study, namely,

$$g(t) = \exp(-((t-t_0)\omega c)^2) \cos(\omega t) \quad (6)$$

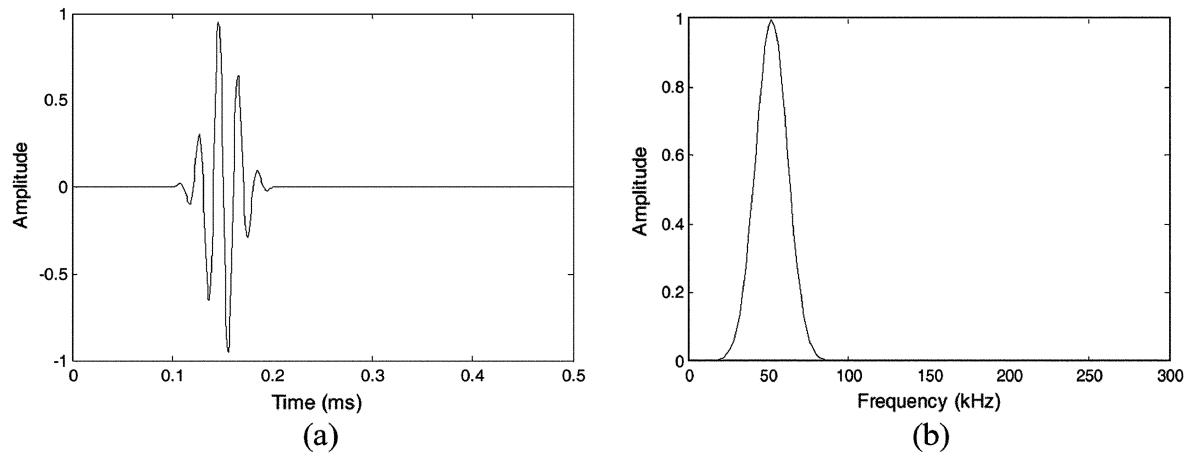


Fig. 1 A Morlet wavelet: (a) waveform, (b) spectrum

This is a Gaussian pulse windowed sine wave covering narrow frequency band at central frequency of ω , with its center locating at t_0 in time domain. Parameter c in Eq. (6) is selected to make the wavelet contain a fixed number of peaks at different ω . Compared to the scaling factor a in Eq. (4) and Eq. (5), ω in Eq. (6) is the inverse of a . With the modified wavelet $g(t)$, wavelet transform in Eq. (5) can be re-written as

$$W_g f(\omega, b) = f(t) * g(t) \quad (7)$$

Given the central frequency ω , $W_g f(\omega, b)$ gives a time domain display of the original signal's components located in the narrow frequency band centered at ω .

The next step is to consider further physical meaning of $W_g f(\omega, b)$. If the excitation signal in Lamb wave inspection is a Dirac function $\delta(t)$, the measured response of the structure is the impulse response $h(t)$. From the signal and system theory (Oppenheim 1986), the convolution of the impulse response $h(t)$ with an arbitrary signal $x(t)$ will be the system's response to $x(t)$, assuming the tested system to be linear and time-invariant. Therefore, if the narrow band burst wave response of the structure is concerned, it can be derived by convoluting the burst wave with $h(t)$. In traditional Lamb wave detection, the input to the system is a Gaussian envelop modulated sinusoidal wave. When this burst wave is in the same form as the wavelet in Eq. (6), the wavelet transform of $h(t)$ will be the burst wave response of the structure. This is the theoretical background for deriving narrow-band response from wide-band response.

Unfortunately, however, the Dirac function is not easy to be produced in practice. To solve this problem we can use a step pulse instead of impulse as the excitation. This step pulse can be generated easily by a general purpose function generator using its low frequency square wave function. When the period of the square wave is very long, it acts as a step pulse in the observing time window. The derivative of structure's response $s(t)$ is then the impulse response $h(t)$ for the given linear and time-invariant system, namely,

$$h(t) = \frac{d}{dt} s(t) \quad (8)$$

With this approach, the response under the input of $g(t)$ specified in Eq. (6) can be calculated,

$$y(t) = h(t) * g(t) \quad (9)$$

In the wideband Lamb wave inspection of structures, the measured waveform is a combination of the guided wave modes at various frequencies. To make a clear observation of the waveform, we can use the modified CWT method introduced in this section to select a narrow frequency band.

3. Experimental results

3.1. Calculation of the narrow band Lamb wave response from the step pulse response

Lamb wave detection usually uses a burst signal as the excitation and the measured results are analyzed to find the internal damages of the structure. The sensitivity of the diagnostic Lamb wave to damages and defects in the structures varies with the type and size of the defects as well as the

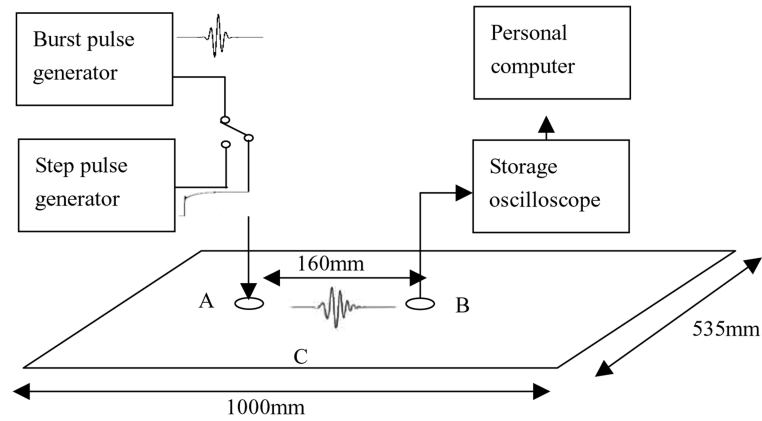


Fig. 2 Sketch of the test setup

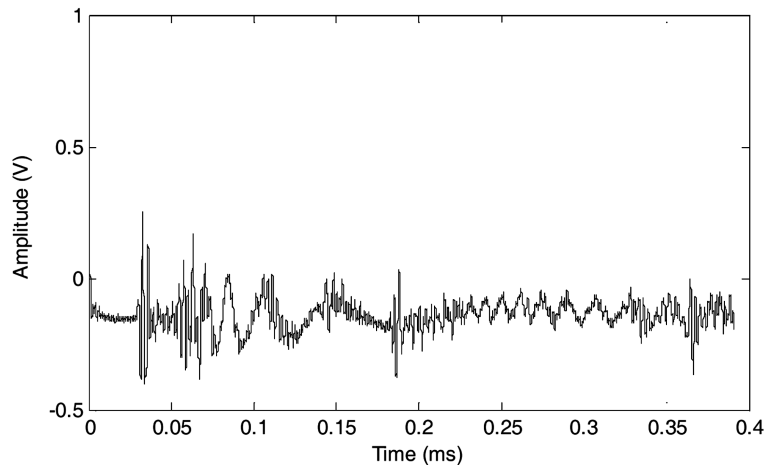


Fig. 3 The step pulse response measured on the aluminum plate

condition of structures. In order to achieve an optimal result, the central frequency of the burst signal needs to be decided. This process depends on both theoretical analysis and experimental investigations. With the proposed method, one can design a step pulse for inspection. By one-time measurement of the wideband step response, the response at a series of frequency band can be acquired by analyzing it with CWT, selecting the central frequency of $g(t)$ in Eq. (6). As a result, the optimal frequency band can be determined for damage detection.

To verify this concept, an experiment was designed. The test setup is given in Fig. 2. A pair of PZT patches were bonded to the upper surface in the center part of a large 2.3 mm thick aluminum plate. The input to the emitting PZT transducer can be selected from two generators: (a) the step pulse and (b) the burst wave with adjustable central frequency. We first measured the step pulse response of the structure and then calculated the narrow band burst wave response from the wideband measurement. The final calculated results were then compared with those directly measured under the excitation of burst signal.

Fig. 3 is the measured waveform by the receiving PZT transducer. Using the CWT method mentioned previously, the burst wave response with the central frequency from 25 kHz to 700 kHz at 20 kHz step

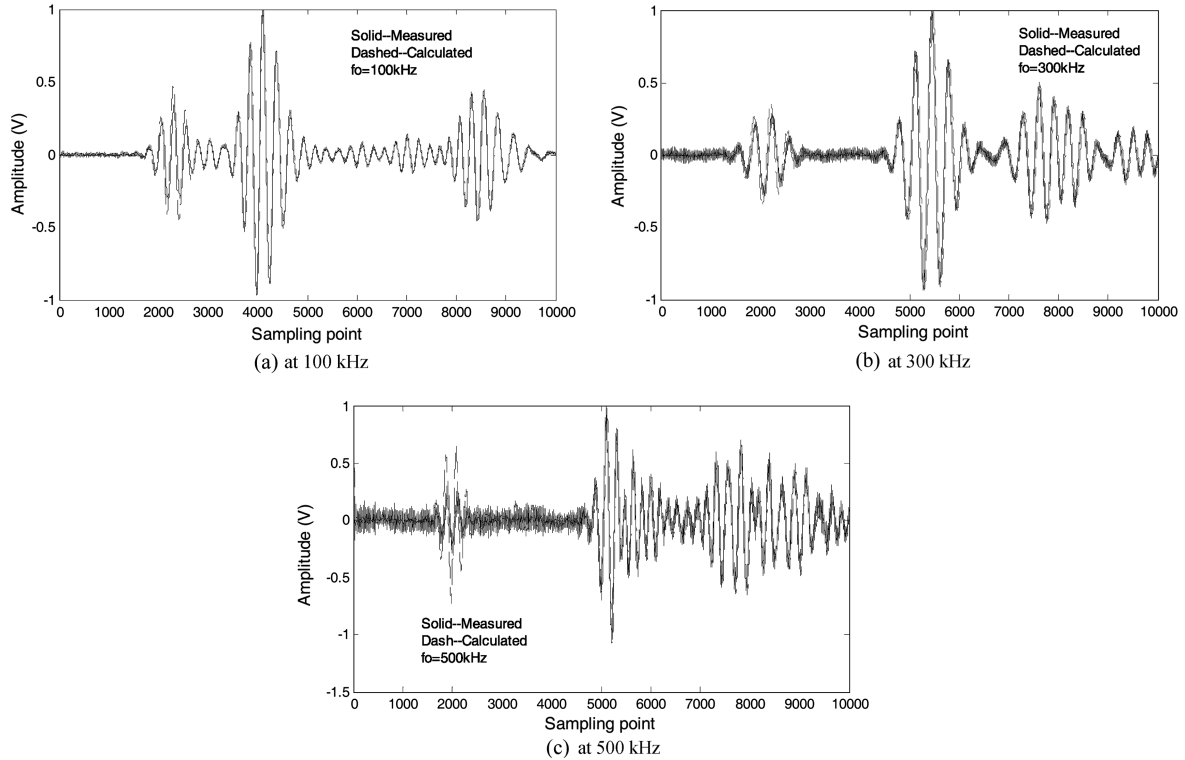


Fig. 4 The comparison of calculated and the measured burst wave response

were calculated. These results are compared to those measured directly under the same burst pulse excitation produced by the burst wave generator. They coincide well with each other. Fig. 4 gives three examples of comparisons of these signals. In these figures, the first wave packet centered at the 2000th point in each plot is not actually the Lamb wave signal. In fact it is the electromagnetic interference coupled from the excitation channel to the receiving channel, so these parts are not considered in the comparison. The rear part after this interference in each plot is the Lamb wave response. With the increment of the central frequency, the figure shows the arriving time of the first Lamb wave packets delays. It is the characteristic of S_0 mode guided wave in plates. The results show by one measurement with the step pulse input, thus, the burst response at a wide range of frequency band can be acquired with the proposed method. In other words, one can determine certain interested frequency band for analysis after the experiment. It should also be noted that, the analyzed result has far less noise in the waveform than the measured one. This is due to the narrow band filtering effect of the CWT method, which make the waveform much clear.

3.2. Analysis of the dispersion effect

Measurement of the dispersion effect of the Lamb wave plays an important role in analyzing the change of structures. Because the step response is a wide band signal and we can acquire the burst wave response from the step pulse response, comparisons of the Lamb wave speed at different frequencies

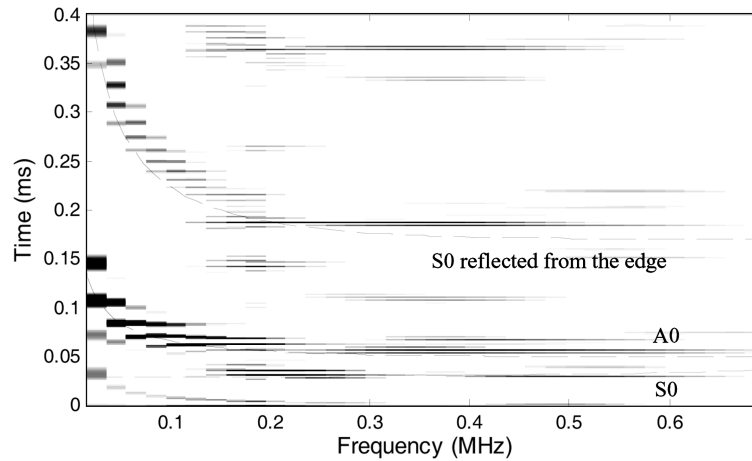


Fig. 5 Time-frequency-magnitude displaying of the dispersion effect

can be carried out. One method is to measure the arriving time of the first Lamb wave packet shown in Fig. 4 and calculate the speed at different frequencies. This method, however, is time consuming and not so accurate since the arriving time of the overlapped signal is not easy to be determined. In the study, the CWT analysis results are plotted at different time and at different central frequencies in 2-D images. In Fig. 5, the horizontal axis is the frequency, while the vertical axis is the time and the gray scale of the image means the signal amplitude. The theoretical group velocity dispersion curves of the aluminum plate are also included in Fig. 5 with dashed lines. The analyzed results have the same trend with the theoretical ones. In the figure, the curve *S₀, reflected from the edge*, means the Lamb wave reflected from the near-edge of the rectangular plate (path A-C-B in Fig. 2). The traveling distance is approximately 400 mm.

3.3. Damage detection

A damage detection experiment was also designed to verify the proposed method. The tested structure was a fiber-glass reinforced epoxy beam shown in Fig. 6. On the surface of the beam, two PZT patches were bonded. One is PZT1 used for excitations and the other is PZT2 used for detections. The step pulse response of the beam without damage was first measured and stored for comparisons. Then a 35 mm pass-through slot, 108 mm apart from PZT2, was made between the propagation path of the Lamb wave in the beam. The measured waveforms before and after the slot was made were given in

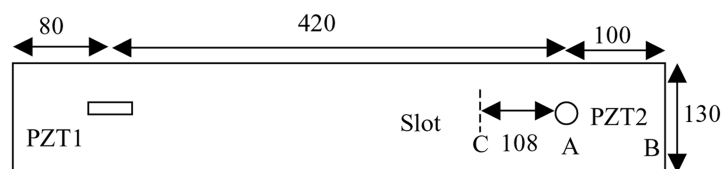


Fig. 6 Test setup of the fiber-glass enforced epoxy beam (unit: mm)

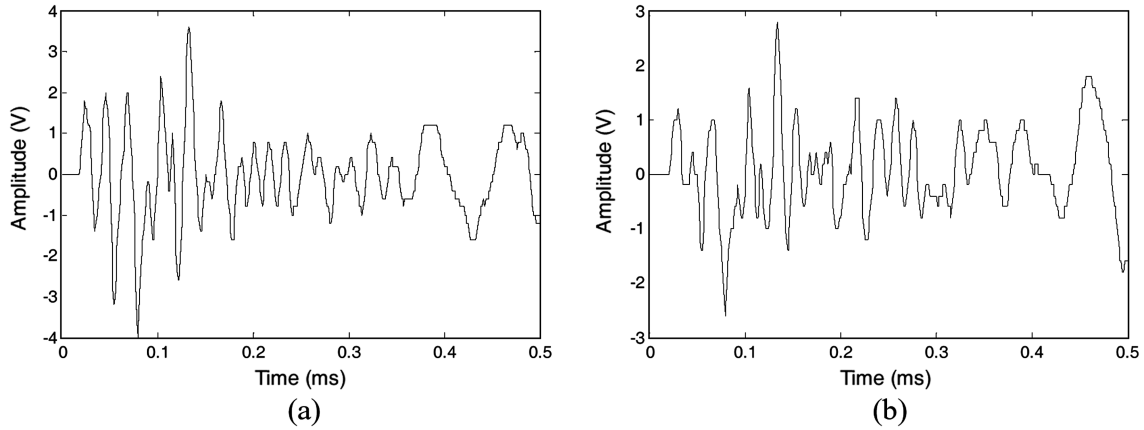


Fig. 7 Measured step response (a) without and (b) with damage

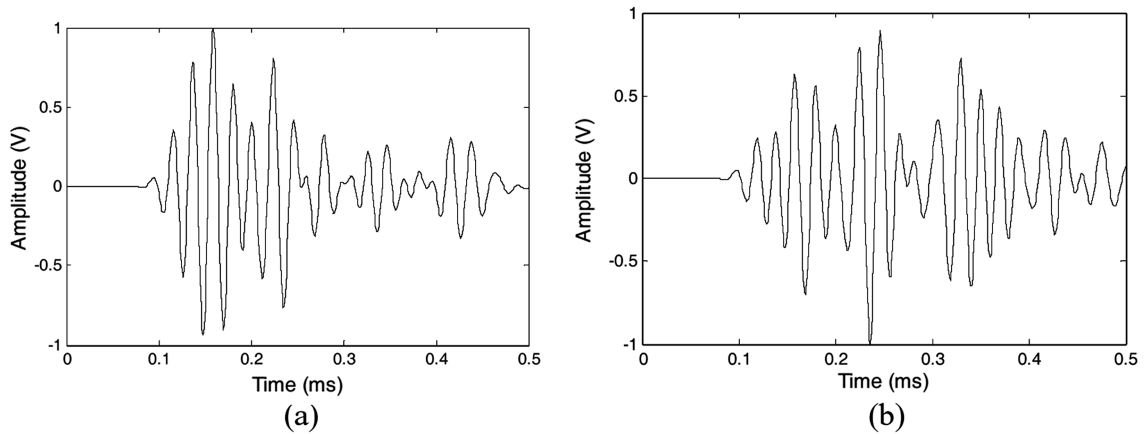


Fig. 8 Burst wave response at central frequency of 40.8 kHz (a) without and (b) with damage

Fig. 7. Obviously, there are some differences in the two waveforms, but the analysis of the difference was not very convenient with traditional methods. Therefore, the measured step response was transformed into narrow band burst wave response using Eq. (8) and Eq. (9), with the central frequency of the burst wave selected from 30 kHz to 60 kHz at interval of 1.2 kHz. Fig. 8 is the time history of the calculated burst response at 40.8 kHz. In these plots, the differences caused by the slot was much more clear. The occurrence of the slot caused the first part of the waveform getting smaller and a new peak appears at the rear of the waveform. There supposed to be two causes of the new peak: the generation of new Lamb wave modes or the reflection from the slot to PZT2. Fig. 9 gives the time-frequency-magnitude display of the CWT analyzed result (similar to Fig. 5). As can be seen that the component in the detected Lamb wave is much clear. This shows that there are two main parts in the original signal at each frequency band. After the occurrence of the slot, there appears a third component between 0.3 ms and 0.35 ms. The new component is mainly caused by the reflection of the existing slot (path A-B-C-A in Fig. 6).

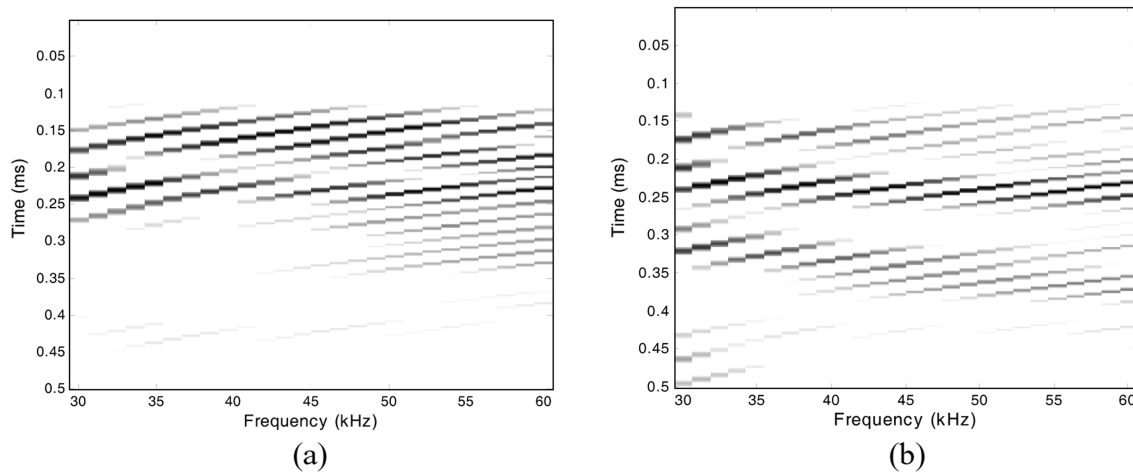


Fig. 9 Time-frequency-magnitude display (a) without and (b) with damage

4. Conclusions

Lamb wave detection in plate structures usually uses narrow band burst waves. In other applications of acoustic wave detection such as measurement of the dispersion curve, acoustic and ultrasonic detection, wide band response is used. This paper proposed a method to retrieve narrow band Lamb wave response from the wideband measurement results. Experimental results show that the proposed method has three possible applications: (1) one-time measurement and multi-frequency band results; (b) dispersion analysis for the group velocity; (c) time-frequency damage diagnosis. It should be noted, however, that the relationship between step response and burst response is based on the assumption that the system is linear-time invariant. When this assumption is not satisfied, the calculated burst wave response will not be the same as the measured one. In this case, the method could be still useful since it acts as a multi-band filter or a time-frequency analyzer, shown by the time-history of the measured waveform in a series of frequency bands.

Acknowledgements

The research is partially supported by the Chinese Natural Science Foundation (Contract No. 50135030).

References

- Abbate, A., Frankel, J. and Das, P. (1995), "Wavelet transform signal processing for dispersion analysis of ultrasonic signals", *Proceedings of IEEE Ultrasonics Symposium*, New York, 751-755.
- Alleyne, D. N. and Cawley, P. (1992), "The interaction of Lamb waves with defects", *IEEE Trans. on Ultrasonics, Ferroelectrics and Frequency Control*, **39**(3), 381-397.
- Alleyne, D. N. and Cawley, P. (1992), "Optimization of Lamb wave inspection techniques", *NDT and E. Int.*, **25**(1), 11-22.

- Alleyne, D. and Cawley, P. (1991), "A two-dimensional Fourier transform method for the measurement of propagating multimode signals", *J. Acoust. Soc. Am.*, **89**(3), 1159-1168.
- Cawley, P. (1997), "Quick inspection of large structures using low frequency ultrasound", *Proceedings of the 1st International Workshop on Structural Health Monitoring*, San Francisco, California, 529-540.
- Chen, C.H., Li, C.P. and Teng, T.L. (2002), "Surface-wave dispersion measurements using Hilbert-Huang transform", *TAO*, **13**(2), 171-184.
- Ellefsen, K. J., Cheng, C. H. and Tubman, K. M. (1989), "Estimating phase velocity and attenuation of guided waves in acoustic logging data", *Geophysics*, **54**(8), 1054-1049.
- Ihn, J. B. and Chang, F. K. (2001), "Built-in diagnostics for monitoring crack growth in aircraft structures", *Proceedings of the 3rd International Workshop on Structural Health Monitoring*, San Francisco, California, 284-295.
- Kessler, S. S., Spearing, S. M. and Soutis, C. (2001), "Optimization of Lamb wave methods for damage detection in composite materials", *Proceedings of the 3rd International Workshop on Structural Health Monitoring*, San Francisco, California, 870-879.
- Lin, M. and Chang, F. K. (2002), "The manufacture of composite structures with a built-in network of piezoceramics", *Composites Science and Technology*, **62**(7), 919-939.
- Lemistre, M. and Balageas, D. (2001), "Structural health monitoring system based on diffracted Lamb wave analysis by multiresolution processing", *Smart Mater. Struct.*, **10**, 504-511.
- Newhouse, V. L., Bilgutay, N. M. Saniie, J. and Furgason, E. S. (1982), "Flaw-to-grain echo enhancement by split spectrum processing", *Ultrasonics*, **20**(2), 58-68.
- Oppenheim, A. V., Willsky, A.S. and Young, I. T. (1983), *Signals and Systems*, Prentice Hall, New York.
- Prosser, W. H., Seale M. D. and Smith, B. T. (1999), "Time-frequency analysis of the dispersion of Lamb modes", *J. Acoust. Soc. Am.*, **105**(5), 2669-2676.
- Paget, C. A., Grondel, S. Levin K. and Delebarre, C. (2003), "Damage assessment in composites by Lamb waves and wavelet coefficients", *Smart Mater. Struct.*, **12**, 393-402.
- Xu, Q. W., Shi, L. H. and Gao C., (2002), "Measurement of the electromagnetic constants of concrete materials by time-domain reflectometry", *Proceedings of International Symp. on Electromagnetic Compatibility*, Beijing, 230-233.
- Viktorov, I. A. (1970), *Rayleigh and Lamb Waves*, Plenum Press, New York.
- Wilcox, P. D., Dalton, R. P., Lowe, M. J. S. and Cawley, P. (1999), "Mode selection and transduction for structural monitoring using Lamb waves", *Proceedings of the 2nd International Workshop on Structural Health Monitoring*, San Francisco, California, 703-712.